

## PDF hosted at the Radboud Repository of the Radboud University Nijmegen

The following full text is a publisher's version.

For additional information about this publication click this link.

<http://hdl.handle.net/2066/21614>

Please be advised that this information was generated on 2017-12-05 and may be subject to change.



# Calculation of Oxygen Pressures in Tissue with Anisotropic Capillary Orientation. II. Coupling of Two-Dimensional Planes

LOUIS HOOFD

*Department of Physiology, Faculty of Medical Sciences, University of Nijmegen, Geert Grooteplein Noord 21, 6525 EZ Nijmegen, The Netherlands*

*Received 30 March 1993; revised 19 July 1994*

---

## ABSTRACT

The mathematical descriptions of oxygen transport in terms of two-dimensional diffusion in planes perpendicular to the capillaries can be coupled for an ensemble of planes to yield a three-dimensional description. In tissue with a distinct orientation of the oxygen supplying structures, the capillaries, this leads to a description of oxygen pressure in a whole tissue volume. Muscle tissue is an example of such tissue. The method allows calculation of oxygen pressure ( $pO_2$ ) at any location in the volume. Tissue volume oxygen status can be assessed by constructing a  $pO_2$  histogram, gathering  $pO_2$ 's at a large number of locations in the tissue.

---

## 1. INTRODUCTION

The complicated task of calculation of oxygen pressures in tissue is simplified considerably when a description in terms of two-dimensional diffusion is allowed [5]. Such a description seems appropriate for tissue with a distinct orientation, like muscle tissue, where the oxygen supplying capillaries run largely in parallel [1]. Under certain conditions, in any plane perpendicular to the capillaries oxygen partial pressure can be described by means of a single mathematical formula. Such a description can serve as a solution by itself [5, 9] or be extended to a three-dimensional description. The parameter constants in the two-dimensional description are derived from the boundary conditions in that plane. These parameters include the oxygen supply area of each individual capillary, which allows calculation of the amount of oxygen withdrawn from the capillary. By coupling consecutive planes, a three-dimensional description can be constructed along the same lines as for the simple Krogh model [10]. In each plane and for each capillary, the oxygen distributed into the corresponding surrounding tissue area is subtracted from the amount in the flowing capillary blood. From the

resulting next-plane  $O_2$  content new capillary  $pO_2$ 's can be calculated. Then, these values can serve as boundary conditions for that next plane. In this way, a number of planes can be overlaid to describe a tissue volume, containing several capillaries (or, capillary segments). Since the two-dimensional solution was explicitly solved for a rectangle or a circle, the resulting tissue volumes of a block and a cylinder are treated most readily. Additionally, tests can be provided concerning the validation of this three-dimensional approach.

## 2. THEORY

### 2.1. PLANE COUPLING

The two-dimensional approach [5] describes oxygen distribution in a plane through a composed quantity, the "driving pressure"  $p^*$ :

$$\mathcal{P} \nabla^2 p^* = \dot{Q}, \quad (2.1)$$

where  $\mathcal{P}$  is oxygen permeability constant of the tissue and  $\dot{Q}$  is its oxygen consumption rate, per tissue volume.  $p^*$  is a composed quantity,  $p^* = p + p_F s$ , where  $p$  is oxygen partial pressure,  $p_F$  is a constant called facilitation pressure [9], and  $s$  is oxygen saturation of the myoglobin (Mb) in the tissue;  $p_F$  depends on Mb concentration and mobility in the tissue. For  $N$  oxygen sources in a flat plane and for the two-dimensional equivalent of (2.1), the formula was derived:

$$p^* = \frac{\dot{Q}}{4\mathcal{P}} \left[ \Phi(\vec{r}) - \sum_{i=1}^N \frac{A_i}{\pi} \ln \left( \frac{|\vec{r} - \vec{r}_i|^2}{r_{ci}^2} \right) \right], \quad (2.2)$$

where  $\Phi$  was termed "background function," a function of location  $\vec{r}$  obeying (2.1) for the plane without sources, and  $A_i, \vec{r}_i, r_{ci}$  are  $O_2$  supply area, location and characteristic measure of the  $i$ th capillary, respectively. This description was in terms of point-like sources and the  $O_2$  supply area  $A_i$  is that of the  $i$ th point source, which is infinitesimally small. When dealing with capillaries, of finite dimensions, part of this  $O_2$  supply flows into the capillary and will be passed to the next plane. The net oxygen release of the  $k$ th capillary has to be found by integration of oxygen flux leaving the capillary across the capillary outline ( $\text{rim } k$ )<sup>1</sup>:

$$\sigma_k O_2 = \oint_{\text{rim } k} J_{nk} dr',$$

<sup>1</sup>Symbols and notation follow the same guidelines as in [5].

where  $\sigma_k O_2$  is the amount of oxygen released into the plane (so, per unit time and per unit tissue length) and  $J_{nk}$  is the oxygen flux perpendicular to the capillary outline and is equal to  $-\mathcal{P} \partial p^* / \partial \vec{n}$ , where  $\vec{n}$  is the vector normal to the outline. The outline is around a capillary area  $A_{ck}$  and we could apply Green's law were it not that the integral is around a singularity, at  $\vec{r} = \vec{r}_k$ . The singularity can be removed by isolating a small area  $A_{\epsilon k}$  around the singularity, with outline rim  $\epsilon$ . Applying Green's law for the remaining "area with a hole":

$$\sigma_k O_2 = \oint_{\text{rim } \epsilon} J_{nk} dr' - \iint_{A_{ck} - A_{\epsilon k}} \mathcal{P} \nabla^2 p^* dA'.$$

Now in the limit for  $\epsilon \rightarrow 0$  the first integral is that of the point source whereas for the second integral the substitution of (2.1) is allowed:

$$\sigma_k O_2 = \dot{Q}(A_k - A_{ck})$$

so that the capillary area has to be subtracted from the point source supply area. This amount of  $O_2$  extracted from the capillary per unit of time and per plane leads to a decrease in capillary  $O_2$ . The  $O_2$  is transported by the flowing blood in the  $z$ -direction perpendicular to the  $x, y$ -plane. Consequently, there is a gradient in blood  $O_2$  flow equal and opposite to the extraction  $\sigma_k O_2$ :

$$\frac{d}{dz}(F_k c_{tk} O_2) = -\sigma_k O_2$$

where  $F_k$  is the capillary blood flow (volume/time) and  $c_{tk} O_2$  the total  $O_2$  content (moles/volume) of the  $k$ th capillary; this total amount encompasses  $O_2$  both free and reversibly bound by chemical reactions with the blood hemoglobin (Hb). Under the assumption that no fluid leaves the capillary, the flow  $F_k$  is independent of plane position  $z$  so that:

$$\frac{d}{dz} c_{tk} O_2 = -\frac{\dot{Q}}{F_k}(A_k - A_{ck}). \quad (2.3)$$

The above derivation is a generalization of that of [10] but it should be noted that in that publication  $F$  is the specific blood flow, i.e., per unit of tissue volume, whereas  $F_k$  here is the blood volume flowing through the  $k$ th capillary only.

## 2.2. CAPILLARY OXYGEN

For the two-dimensional solution [5] only the value of the  $k$ th capillary  $pO_2$ ,  $p_{ck}$ , had to be known, but here also its relation to the  $O_2$  content  $c_{tk}O_2$  has to be found. Most of the capillary oxygen is contained in the erythrocytes so that it is straightforward to take  $p_{ck}$  as the erythrocyte  $pO_2$ . Due to intracapillary transport, however, plasma  $pO_2$  will be lower than erythrocyte  $pO_2$  and consequently average capillary  $pO_2$ ,  $\bar{p}_{ck}$ , will be also. The total capillary  $O_2$  content is expressed as:

$$c_{tk}O_2 = \bar{\alpha}_k \bar{p}_{ck} + \bar{B}_k s_{ck}, \quad (2.4)$$

where  $\alpha$  is oxygen solubility,  $B$  is oxygen binding capacity, and  $s_c$  is Hb oxygen saturation. The overbars indicate average values, averaged over the whole capillary, erythrocyte, and plasma, and the index  $k$  indicates the  $k$ th capillary. These values may be different for each capillary since hematocrit values can be different and all quantities have to be evaluated for each respective erythrocyte/plasma mixture. The  $O_2$  binding groups in the hemoglobin molecule are the four heme groups, so when all these groups are available for oxygen (none blocked by, e.g., CO or oxidation) the oxygen binding capacity  $B_k$  is equal to the heme concentration, i.e., four times the average Hb concentration of the  $k$ th capillary. The saturation  $s_{ck}$ —the erythrocyte saturation—is related to  $p_{ck}$  through the equilibrium relation the oxygen dissociation curve (ODC) assuming chemical reactions to be fast (these are of the order of milliseconds [2]). There are several equations available for the description of this chemical equilibrium, the easiest one being the so-called Hill formula [4]:

$$s_c = \frac{p_c^n}{p_{50,c}^n + p_c^n}, \quad (2.5)$$

where  $p_{50,c}$  is the Hb half-saturation  $O_2$  pressure and  $n$  is called the Hill constant. The subscripts  $k$  have been dropped since the equation is general, holding for all capillary blood. There is vast literature about the topic of Hb- $O_2$  interaction. Depending on capillary blood conditions, such as  $pCO_2$ ,  $pH$ , temperature, etc., the half-saturation pressure can be different for each capillary situation whereas such differences for  $n$  are so small that they can be neglected. The Hill formula is an empirical equation lacking chemical background but describes most ODCs very well above  $\sim 10\%$  saturation. For the remaining part, extensions by other formulations are available [2, 13, 14] but they rarely will be needed because capillary saturations in this range are quite unphysiological.

When elaborating (2.3), the difference between the  $\bar{p}_{ck}$  of (2.4) and "capillary"  $p_{ck}$  as in (2.5) is irrelevant if that difference is independent of  $z$ . In other words,  $p_{ck} - \bar{p}_{ck}$  may be different for different capillaries but that does not matter when it is a constant along the capillary trajectory for any particular capillary. In that case  $d\bar{p}_{ck}/dz$  is equal to  $dp_{ck}/dz$  and (2.3), (2.4) can be combined:

$$\left(1 + p_{\beta,k} \frac{ds_c}{dp_c}(p_{ck})\right) \frac{dp_{ck}}{dz} = - \frac{\dot{Q}}{\bar{\alpha}_k F_k} (A_k - A_{ck}), \quad (2.6)$$

where  $p_{\beta,k} = \bar{B}_k / \bar{\alpha}_k$  is the pressure equivalent of the amount of chemically bound  $O_2$  present in 100% saturated blood. Equation (2.6) relates oxygen supply to axial gradient in capillary pressure, i.e., between the planes.

In the calculation algorithms for the parameters in (2.2),  $r_{ci}$  was taken as the effective capillary radius,  $r_{ci}^2 = A_{ci} / \pi$ . Note, however, that this does not imply that the capillary outline is circular. Instead, (2.3) and (2.6) are derived generally. Moreover, capillary outlines are allowed to be different in each plane.

### 3. CALCULATION ALGORITHMS

#### 3.1. LAYER STEP

For solving a particular situation, it is obvious that for each capillary a value of  $p_{ck}$  must be assumed in one of the planes. Say, that for all capillaries this is the plane at  $z = 0$ . In each consecutive plane, the capillary values follow from (2.6). Going from the plane at  $z = z_m$  to  $z = z_{m+1}$  the left side can be easily integrated and as a first approximation the right side can be considered (approximately) constant:

$$\begin{aligned} (p_{ck} + p_{\beta,k} s_{ck}) \Big|_{z=z_{m+1}} \\ \approx (p_{ck} + p_{\beta,k} s_{ck}) \Big|_{z=z_m} \\ - \frac{\dot{Q}}{\bar{\alpha}_k F_k} \left( \left| \cdot A_k \right|_{z=z_m} - A_{ck} \right) (z_{m+1} - z_m), \end{aligned} \quad (3.1)$$

where the relation in fact is for  $p_{ck}$  because of its one-to-one relationship with  $s_{ck}$ , the ODC. When  $A_k$  is overestimated by taking the value at  $z = z_m$ ,  $p_{ck}$  will be estimated too low at  $z = z_{m+1}$ . Such low  $p_{ck}$  results in less supply, i.e., too low a value calculated for  $A_k$  in that plane. Then, according to (3.1) the next pressure drop is underestimated. Consequently, this scheme with a first-order approximation for

$A_k$  is expected to be sufficient. It can be improved by repeating the calculation of (3.1) now with an averaged value of  $A_k$ :

$$\begin{aligned} & (p_{ck} + p_{\beta,k} s_{ck}) \Big|_{z=z_{m+1}} \\ & \approx (p_{ck} + p_{\beta,k} s_{ck}) \Big|_{z=z_m} \\ & - \frac{\dot{Q}}{\bar{\alpha}_k F_k} \left( \frac{1}{2} A_k \Big|_{z=z_m} + \frac{1}{2} A_k \Big|_{z=z_{m+1}} - A_{ck} \right) (z_{m+1} - z_m), \end{aligned}$$

and this procedure might be iterated. Whether and how many iterations are needed will depend on the step size  $z_{m+1} - z_m$ .

### 3.2. ELABORATION OF THE LAYER STEP

The layer step yields a formula for a combination of  $p_{ck}$  and  $s_{ck}$  in the plane at  $z = z_{m+1}$  (see (3.1)) which generally can be written as:

$$p_{ck} + p_{\beta,k} s_{ck} = G_k. \quad (3.2)$$

Commonly, the term  $p_{\beta,k} s_{ck}$  will be the larger term and an iterative method should be set up correcting  $s_{ck}$ . However, this quantity is bounded between 0 and 1 and corrections either must be restricted to that range or applied to a mathematically transformed value. An appropriate transformation seems to be

$$p_c = p_{50,c} \exp(t) \quad (3.3)$$

and a corresponding expression for  $s_c$  according to the ODC, e.g., (2.5). Initial estimates  $p_{ck}^{(0)}, s_{ck}^{(0)}, t^{(0)}$  can be found by using the values of the former plane (at  $z = z_m$ ) and the estimates of the next step come from linearization of (3.2), worked out in terms of (2.5):

$$\left\{ p_{ck}^{(j)} + p_{\beta,k} n s_{ck}^{(j)} (1 - s_{ck}^{(j)}) \right\} \Delta t^{(j)} = G_k - p_{ck}^{(j)} - p_{\beta,k} s_{ck}^{(j)},$$

allowing calculation of  $\Delta t^{(j)} = t^{(j+1)} - t^{(j)}$ . According to (3.3) the next-step pressure is found from

$$p_{ck}^{(j+1)} = p_{ck}^{(j)} \exp(\Delta t^{(j)}),$$

but it was found that the procedure becomes even faster when the exponent is linearized:

$$p_{ck}^{(j+1)} = \begin{cases} p_{ck}^{(j)} (1 + \Delta t^{(j)}) & \Delta t^{(j)} > 0 \\ \frac{p_{ck}^{(j)}}{1 - \Delta t^{(j)}} & \Delta t^{(j)} < 0. \end{cases}$$

Also note, that the above formulas are applicable for other schemes of the relationship between  $p_c$  and  $s_c$  than stated in (2.5) if an appropriate value for  $n$  is used [13, 14]. Furthermore, iteration may be speeded up by combining the steps for calculation of  $p_{ck}^{(j+1)}$  and averaging  $A_k$  over the planes at  $z = z_m$  and  $z = z_{m+1}$ .

#### 4. RESULTS OF AN EXEMPLARY CASE

As a calculation example, a tissue block was considered with parallel capillaries running from bottom ( $z = 0$ ) to top plane ( $z = z_M$ ) where capillary location in each plane was according to the situation of Figure 1. The cross-section is square and distances will be expressed as fractions of the width/height (0–1). The square field was divided into four zones of equal size with different conditions of capillary spacing/capillary flow, as indicated by the letter combinations in Figure 1. The first letter **E** or **H** indicates equally or heterogeneously spaced

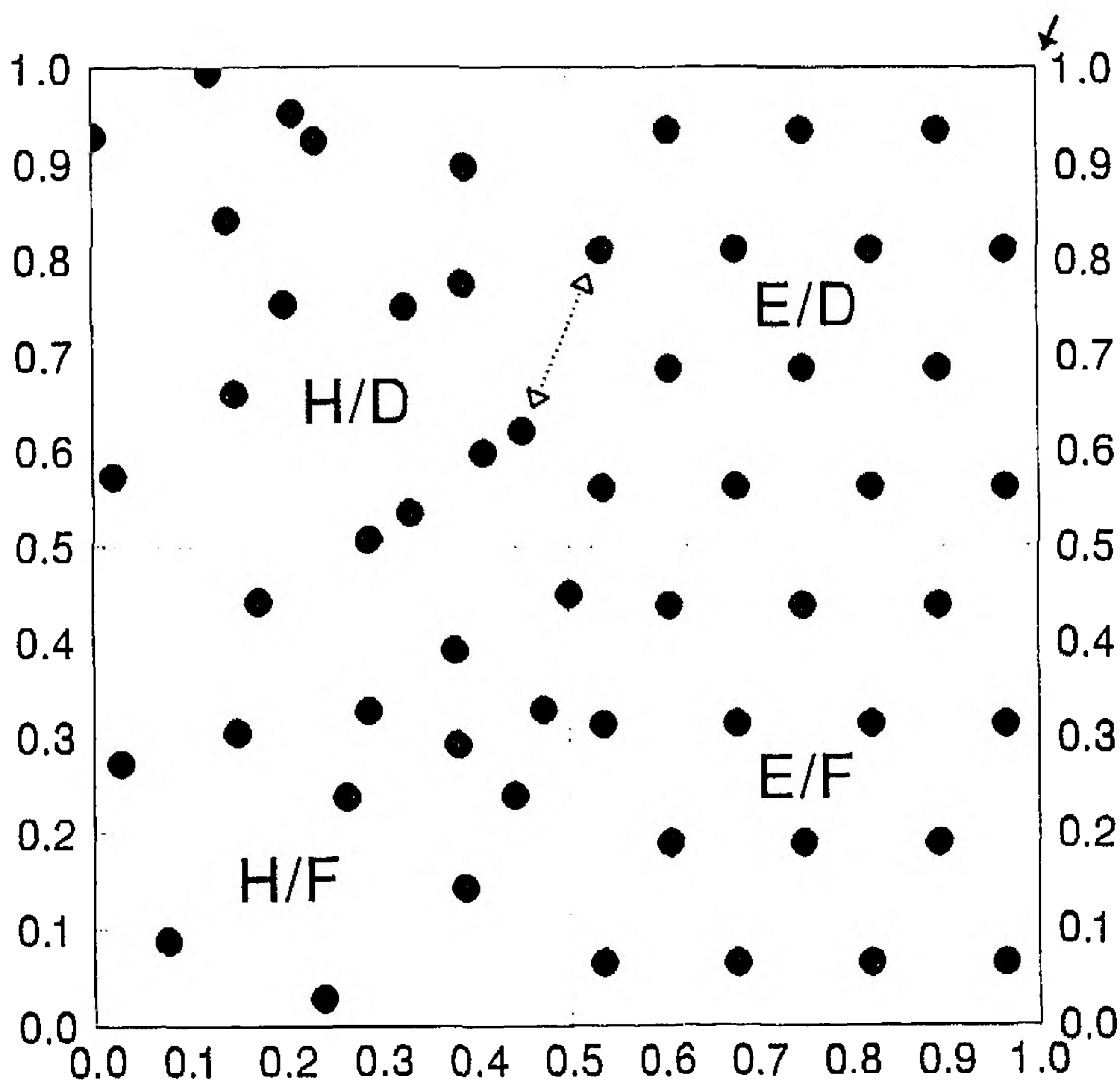


FIG. 1. Capillary locations of the example, a square field of four square zones with different capillary properties as indicated by the two-letter coding. The first letter indicates equal (**E**) or heterogeneous (**H**) capillary spacing, the second identical flow (**F**) or randomly distributed flow (**D**). Distances are given as fractions of the maximum. The thick arrow top right is the viewpoint direction of Figure 2; the dotted arrow points to the two capillaries indicated there.



capillaries and the second letter **F** or **D** identical ( $F_k$  equal to the average value of all capillaries) or randomly distributed capillary flow respectively. The example is to elucidate some effects of heterogeneities in capillary spacing and capillary flow. The equally spaced capillaries were placed in a filled hexagonal grid whereas the heterogeneous distances were as for realistic rat heart [9] (combined with a square side of  $152 \mu\text{m}$ ). Random flow was distributed with a standard deviation of 0.2 and all the other capillary data ( $r_{ck}$ , initial  $p_{ck}$ ,  $p_{50,ck}$ ,  $p_{\beta,k}$ ) were identical for each capillary. There was no facilitation by myoglobin and no difference between capillary and capillary-rim pressure ( $p_F = 0$  and all  $\gamma_k = 0$ ; see [5]). The remaining data are summarized in Table 1 and are taken also from [9], combined with a layer spacing of  $5 \mu\text{m}$ . The  $\dot{Q}/\bar{\alpha}_k F_k$  needed for the evaluation of (3.1) come from combination of the  $\dot{Q}/\mathcal{P}$  needed for the calculations within each plane and the dimensionless parameter  $\mathcal{P}z_M/(\alpha F)$ , where  $\alpha F = \bar{\alpha}_k F_k$ , which was identical for each capillary.

#### 4.1. OXYGEN PRESSURE IN EACH PLANE

The resulting  $p\text{O}_2$  fields were calculated for two planes, at  $z = 0$  (high  $p\text{O}_2$ ) and at  $z = z_M$  (low  $p\text{O}_2$ ), reached in 60 equidistant steps ( $M = 60$ ). In-field values were calculated using (2.2) as described in [5], whereas the steps were taken according to (3.1). Both  $p\text{O}_2$  fields are shown in Figure 2, together with the capillary  $p\text{O}_2$ s indicated as solid dots—note, that these capillary  $p\text{O}_2$ 's in the top profile are identical ( $p_{ck} = 2.5$ ). Pressure drop between the planes is different for different supply-area/flow combinations; a good example is seen for the capillaries indicated by the arrow in the lower ( $z = z_M$ ) field. In contrast, in the E/F region seen at the left the drop is equal for each capillary.

#### 4.2. TISSUE VOLUME OXYGEN HISTOGRAM

Usually, the oxygen status of a whole piece of tissue is expressed in terms of a  $p\text{O}_2$  histogram, where the oxygen pressure is sampled at a

TABLE 1

Parameter Values Used for the Calculations of Figure 2 and Figure 3\*

Quantity	$r_{ck}$	$\dot{Q}/\mathcal{P}$	$\mathcal{P}z_M/(\alpha F)$	$p_{ck,z=0}$	$p_{\beta,k}$	$n$
Unit	$l$	$\text{p}\cdot l^{-2}$	—	p	p	—
Value	0.0158	115.5	30	2.5	169	2.7

\* All values are relative to field width (length, unit  $l$ ) and  $p_{50,c}$  (pressure, unit p);  $\mathcal{P}z_M/(\alpha F)$  and  $n$  are dimensionless. Dimensional values of  $r_{ck}$  and  $p_{ck,z=0}$  were  $2.4 \mu\text{m}$  and  $12.5 \text{ kPa}$  respectively.

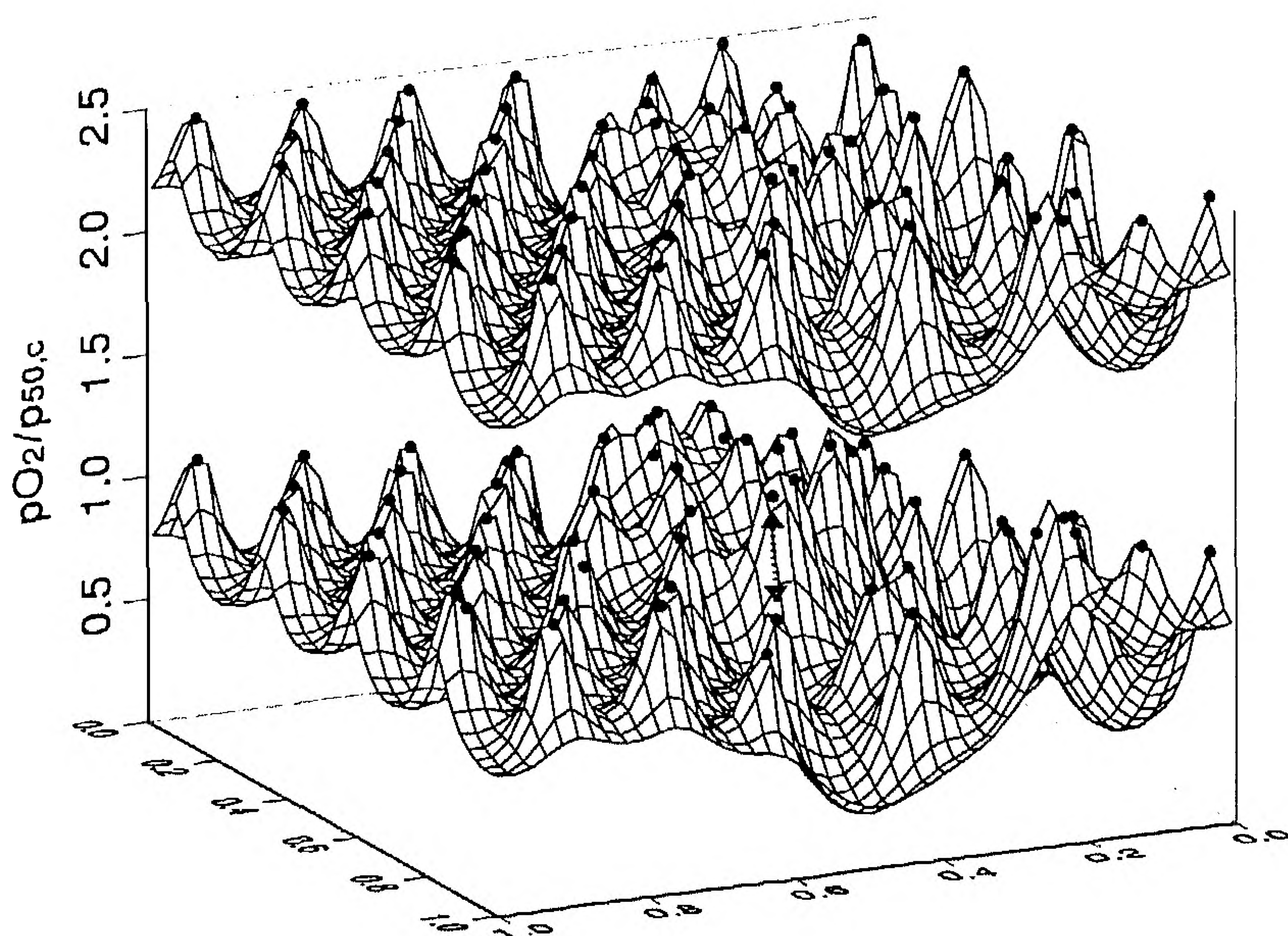


FIG. 2. Tissue  $pO_2$  (vertical axis; relative units) fields calculated for the capillary arrangement of Figure 1; base plane shown with the same axes as in this figure (E/D zone in front); viewpoint  $65^\circ$  in (see solid arrow in Figure 1) and  $15^\circ$  above the  $x, y$ -plane. Top field is for homogeneous starting capillary  $pO_2$  ( $z = 0$ ); bottom field is for end-capillary conditions ( $z = z_M$ ). Solid dots indicate capillary pressures; the arrow points to a clearly visible case of difference between end pressures.

number of locations and gathered into  $pO_2$  classes. This can be simulated here by calculating  $pO_2$  in a cubic grid with a lattice distance equal to the distance between the planes, i.e., identical square grid in each plane. This resulted in 56120 grid points (grid points inside a capillary were omitted, of course). Values were gathered in classes of  $0.1p_{50,c}$  width and shown as fraction  $f$  of the total number in Figure 3. Also, the cumulative histogram (Cum) is shown as black dots interconnected by solid lines; these dots indicate the percentage of values calculated below the corresponding  $pO_2$  threshold. This type of histogram is utilized in literature as well. In both ways, a good impression can be obtained of the oxygen status of the tissue block.

## 5. DISCUSSION

The present method provides a straightforward way to calculate  $pO_2$  in a whole volume. The basis for this calculation is the two-dimensional method [5] and the individual planes are coupled as described above.

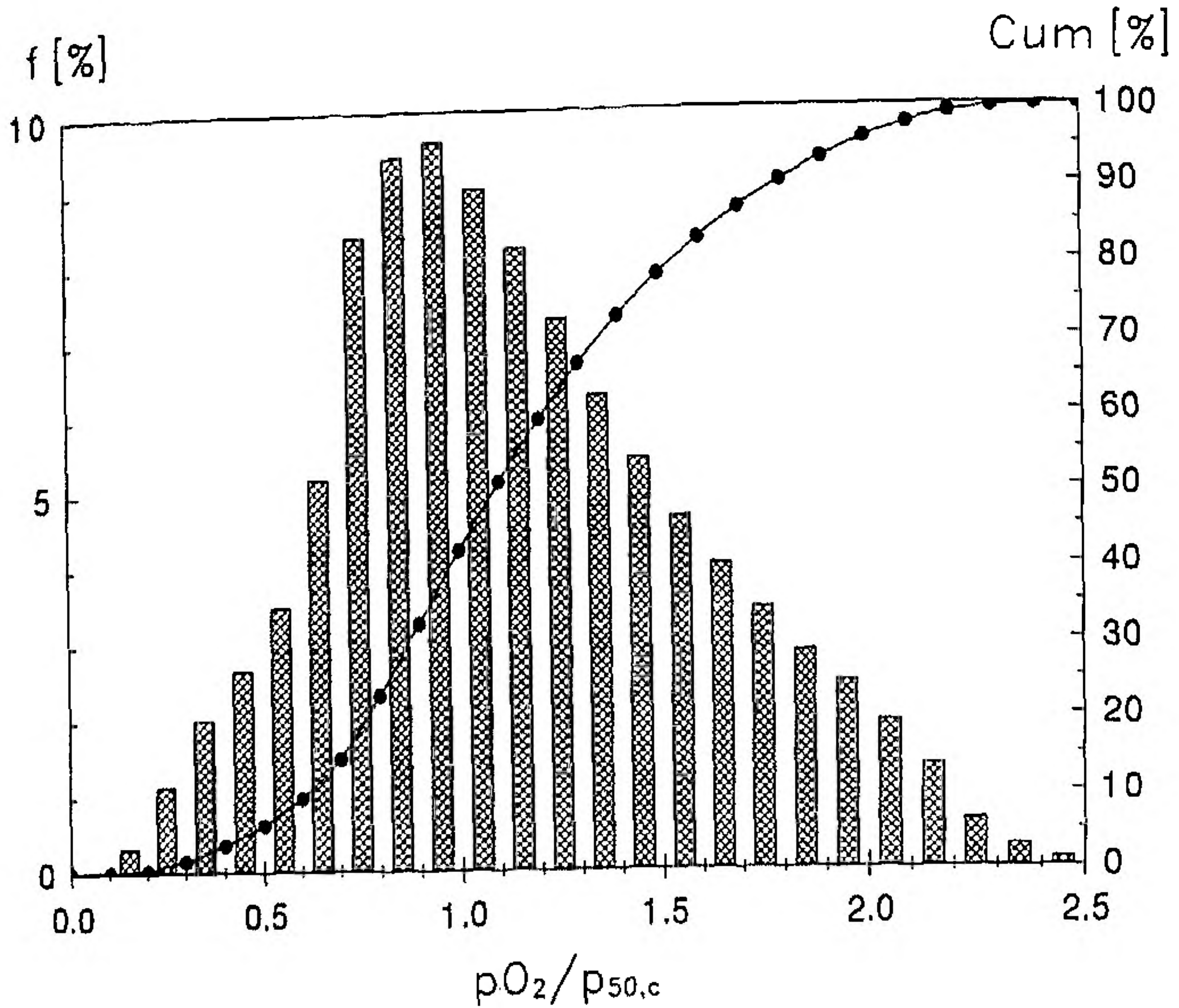


FIG. 3.  $pO_2$  histogram calculated for the example at 56120 locations in the tissue block. Bars are frequency ( $f$ ; left axis) of occurrence of tissue  $pO_2$  in the classes as shown on the horizontal axis (relative units); dots connected by solid line are cumulative frequency (Cum; right axis).

The assumption involved, consequently, is that the influence of adjacent planes on the calculation within a plane is negligible. It comes down to a constraint already stated for the two-dimensional solution, that the term  $\partial^2/\partial z^2$  in the Laplacian of (2.1) must be negligible. This can be judged numerically by approximating the second derivative  $\partial^2 p^*/\partial z^2$  at  $(x, y, z = z_m)$  by the corresponding difference equation. This  $\partial^2 p^*/\partial z^2$  is a part  $fr$  of  $\nabla^2 p^*$  and  $\nabla^2 p^*$  is equal to  $\dot{Q}/\mathcal{P}$  so that

$$fr = 2 \frac{\mathcal{P}}{\dot{Q}} \left| \frac{(z_m - z_{m-1})p_{m+1}^* - (z_{m+1} - z_{m-1})p_m^* + (z_{m+1} - z_m)p_{m-1}^*}{(z_m - z_{m-1})(z_{m+1} - z_{m-1})(z_{m+1} - z_m)} \right|,$$

where  $p_m^*$  is the value evaluated at  $(x, y, z_m)$ , respectively. The fraction  $fr$  should have a negligible influence on the calculations; consequently,  $fr$  should be small. When tissue  $pO_2$  largely follows capillary  $pO_2$  (only gradual shifts in oxygen supply areas and only little desaturation of the myoglobin in the tissue) the estimation of  $fr$  can be restricted to the capillary  $pO_2$ s ( $fr_c$ ). In the above example, the maximum value found was 0.13; this occurs in the  $(z = 0)$ -plane, and after that initial plane both the maximum (0.035 for  $z = z_5$ ) and the average value rapidly

decrease so that in large regions of the tissue block  $fr$  was far below 1%. For  $fr_c$ , a formula can be derived using (2.6):

$$fr_{ck} = \mathcal{P} \dot{Q} \left( \frac{A_k - A_{ck}}{\bar{\alpha}_k F_k} \right)^2 \frac{P_{\beta,k} \left| \frac{d^2 s_c}{dp_c^2} \right|}{\left( 1 + P_{\beta,k} \frac{ds_c}{dp_c} \right)^3} \Bigg|_{p_c = p_{ck}}$$

and indeed  $fr_c$  will become small when the ODC becomes involved, i.e.,  $P_{\beta,k}(ds_c/dp_c)$  is large. Also, where the ODC is approximately linear,  $s_c \approx s_{ck} + \{ds_c/dp_c(p_{ck})\}(p_c - p_{ck})$ , the second derivative  $d^2s_c/dp_c^2$  is almost zero and consequently  $fr_c$  is. Therefore, especially for the physiologically interesting range where the Hb is active the above method seems to be appropriate.

The picture is not complete for a situation where capillaries are not straight and parallel to the  $z$ -direction, or when they start or end in one of the planes between  $z = 0$  and  $z = z_M$ . There is no constraint in the above derivation that capillary locations must be the same for all planes, so slanting, tortuous, and even branching capillaries and capillary pieces of limited length are not excluded beforehand [6]. The constraint still is that the term  $\partial^2/\partial z^2$  in the Laplacian can be neglected. This should be tested for the whole piece of tissue under consideration.

For capillaries branching from an arteriole (or draining into a venule) the situation is even more complicated because of the presence of the larger blood vessel, which can extend in any direction and might distribute oxygen itself. The arteriole has the highest  $pO_2$  so gives rise to a local large value of  $\partial^2 p/\partial z^2$  but that is not so relevant since the vessel is at that very location distributing oxygen. So, capillary ends should be handled with some caution, more so since the high values of  $fr_c$  are expected there, as found in the above example. Possibly, the highest  $pO_2$  values found in the calculations should be disregarded. This concerns only a small portion of the total tissue, as can be seen from the example, Figure 3, where the tissue fractions close to the highest pressure of  $2.5p_{50,c}$  are very small.

It is just one of the features of the treatment presented here that all capillary data can be different for the individual capillaries. Not only capillary location  $\vec{r}_i$  but also its outline, flow, Hb content (hematocrit), initial  $pO_2$  drop ( $\gamma_k$ , see [5]) and internal conditions determining  $p_{50,ck}$  (like  $pCO_2$  and  $pH$ ) can be chosen individually. Outline,  $\gamma_k$ , and internal conditions can be different even for each different plane. This opens the way for investigation of the effects of capillary redistributions of flows and erythrocytes on tissue  $pO_2$ .

The method is semi-analytical, where the  $pO_2$  within a plane is directly described by mathematical formulas [(2.2)] and the planes are coupled numerically. In order to solve the situation for a whole piece of tissue, first the conditions of each individual plane must be calculated, i.e.,  $\Phi(\vec{r}_0)$  and  $A_k$  must be known, where  $\vec{r}_0$  is any location in the plane. This means that the number of calculations is restricted to the number of capillaries plus one, where a purely numerical method would need a much denser grid in each plane (certainly more than 100 grid points per capillary [6]). The block is the readiest form of tissue piece especially for calculation of a  $pO_2$  histogram since it is apt to be overlaid with a cubic grid. It is to be expected that a regular grid is random with respect to the tissue since capillary locations are not regular in a tissue. When it is regular nevertheless, as in the above example in the E/F and E/D zones, the grid spacing must be chosen cautiously to avoid calculation of  $pO_2$  systematically at the same distance of the capillaries, as is done in the above example by choosing the quotient of grid spacing and capillary distance equal to 0.2647. In judging the effects of heterogeneity of capillary spacing this should be—and has been [5]—a point of concern.

Since flow can be chosen negative, modeling of countercurrent flows is also possible [7]. This was done in literature also using different models or configurations [12]. There is a problem in choosing the boundary conditions since now a low value of capillary  $pO_2$  must be found in the initial ( $z = 0$ ) plane and will increase in each following plane such that it ends at the correct, e.g., arterial, value. This may be a bit tricky because a small overestimation of this initial  $pO_2$  can lead to “exploding” (increasing very fast) capillary  $pO_2$ 's in the last planes. The reason is that with high  $pO_2$  the Hb becomes loaded with oxygen and can store hardly any more. This causes the next-plane  $pO_2$  to be much higher, which in turn leads to a high supply area so a high flux from the capillary; the high  $O_2$  outflow implies a higher added amount for the next plane. It is just the opposite of the argument following (3.1). For oxygen pressures staying within the physiological range, one should always be able to find an appropriate initial value.

Subtracting  $A_{ck}$  from  $A_k$  as in (2.3) seems an unimportant correction because the total space occupied by capillaries is mostly only a small fraction of the tissue volume. This might be true considering the tissue, but it can be important for the capillaries. Equation (2.2) allows for very small individual capillary  $O_2$  supply areas  $A_k$ —these can even become negative [5]. Let us assume a supply area  $A_k$  that is half the size of the capillary area  $A_{ck}$ . Then, neglecting  $A_{ck}$  in (2.3) would predict decreasing capillary  $pO_2$  whereas actually this value would increase.

The coupling of planes can be considered as an extension of the method of [10]. Plane coupling can be done for any two-dimensional

description (see [12]). Here, it is laid out in terms of capillary oxygen supply areas  $A_k$  and it could be combined with any two-dimensional method that allows calculation of such supply areas. The net  $O_2$  release is calculated also considering the actual capillary shape [(2.3)]. Also, the further derivations are quite general, allowing for differences between erythrocyte and apparent capillary  $pO_2$ s ( $\bar{p}_{ck}$  and  $p_{ck}$ ). An area might be negative which would imply real oxygen shunting, from adjacent capillaries to the one under consideration [3]. Capillary flow cannot only be heterogeneous but also countercurrent flow is allowed, as done by [11].

In the example of Figures 1 and 2, heterogeneity in capillary flow leads to heterogeneity in tissue  $pO_2$ . This is best seen in the E/D zone of Figure 1. In Figure 2, this is the front middle part, where the top profile starts homogeneous and bottom profile ends heterogeneous. Heterogeneity in  $pO_2$ , however, is much less than in the adjacent zones with heterogeneous capillary locations. Actually, there is a mitigating effect. A rapidly decreasing capillary  $pO_2$ , either due to a large supply area or to low blood flow, will lead to a smaller supply area  $A_k$  in the following planes and consequently to less oxygen release there. Eventually, the resulting heterogeneity in capillary  $pO_2$  will increase only slightly [7,8]. In the example of Figure 2, the capillaries indicated by the arrow have very different supply areas in the starting plane (top profile); that of the front capillary is 58% larger than the other one. In the bottom plane, it is only 24% larger. Capillary  $pO_2$ 's both start at  $2.5p_{50,c}$ , half-way they differ by  $0.29p_{50,c}$  and in the bottom plane by slightly more,  $0.32p_{50,c}$ . Half the bottom-plane  $pO_2$  difference,  $0.16p_{50,c}$ , is reached in the first 15% of the capillary length. When starting from heterogeneous capillary  $pO_2$ 's (in the top plane) the deviation in  $pO_2$  decreases, as found by others [3, 11, 12].

Summarizing, the method presented here is considered to be a powerful tool in the modeling of oxygen transport to tissue. It is directly applicable to tissue models with straight and parallel capillaries, while the other capillary data can be chosen freely. Several extensions to other situations are open (see also [5]) but these should be considered individually.

## APPENDIX: NOMENCLATURE

$A_i$	$A_k$	capillary supply area
$A_{ci}$	$A_{ck}$	capillary cross-sectional area
$A_{\varepsilon k}$		infinitesimal area
$B_k$		oxygen binding capacity of hemoglobin
$c_{tk}O_2$		total capillary oxygen content

$F_k$	capillary blood flow
$fr$	estimated three-dimensional error in Laplacian
$fr_c$ $fr_{ck}$	capillary estimate of $fr$
$G_k$	equivalent combined pressure $O_2 + Hb$
Hb	hemoglobin
$J_{nk}$	flux across capillary outline
$M$	number of layers
Mb	myoglobin
$N$	number of capillaries
$n$	Hill constant
$\vec{n}$	vector normal to capillary outline
ODC	oxygen dissociation curve of hemoglobin
$\mathcal{P}$	oxygen permeability constant
$p$	oxygen partial pressure, $pO_2$
$p_{50,c}$ $p_{50,ck}$	hemoglobin half-saturation pressure
$p_c$ $p_{ck}$	capillary oxygen pressure
$p_F$	facilitation pressure
$p_{\beta,k}$	equivalent hemoglobin pressure
$p^*$	oxygen driving pressure
$\dot{Q}$	oxygen consumption rate
$\vec{r}$	two-dimensional coordinate vector
$\vec{r}_0$	reference location in plane
$r_{ci}$	effective capillary radius
$\vec{r}_i$ $\vec{r}_k$	capillary location
rim $k$	capillary rim
rim $\varepsilon$	outline of infinitesimal area
$s$	myoglobin saturation
$s_c$ $s_{ck}$	hemoglobin saturation
$t$	transformed variable ((3.3))
$x$ $y$ $z$	cartesian coordinates
$z_m$	location of the $m$ th plane

### GREEK SYMBOLS

$\alpha_k$	oxygen solubility
$\gamma_k$	pressure drop proportionality factor
$\Delta t$	step in $t$
$\varepsilon$	infinitesimal distance
$\sigma_k O_2$	capillary oxygen release per plane
$\Phi(\vec{r})$	background function

### SUPERSCRIPTS

(0) (j) (j+1)	iteration index
' "	dummy variable
overbar	average value

## REFERENCES

- 1 S. Batra and K. Rakušan, Capillary length, tortuosity, and spacing in rat myocardium during cardiac cycle, *Amer. J. Physiol.* 263:H1369–H1376 (1992).
- 2 S. Bouwer, Facilitated Oxygen Diffusion through Hemoglobin Solutions. Measurement of Diffusion and Reaction Parameters, Dissertation Thesis, University of Nijmegen, The Netherlands, 1987.
- 3 M. L. Ellsworth, A. S. Popel, and R. N. Pittman, Assessment and impact of heterogeneities of convective oxygen transport parameters in capillaries of striated muscle: Experimental and theoretical, *Microvasc. Res.* 35:341–362 (1988).
- 4 A. V. Hill, The possible effects of the aggregation of the molecules of haemoglobin on its dissociation curves, *J. Physiol.* 40:iv–vii (1910).
- 5 L. Hoofd, Calculation of oxygen pressures in tissue with anisotropic capillary orientation. I. Two-dimensional analytical solution for arbitrary capillary characteristics, this volume.
- 6 L. Hoofd, Updating the Krogh model—assumptions and extensions, in *Oxygen Transport in Biological Systems*, Society for Experimental Biology Seminar Series 51, S. Egginton, and H. F. Ross, eds., Cambridge University Press, Cambridge, 1992, pp. 197–229.
- 7 L. Hoofd and Z. Turek, The influence of flow redistributions on the calculated  $pO_2$  in rat heart tissue, in *Oxygen Transport to Tissue-XV*, Advances in Experimental Medicine and Biology, vol. 345, P. Vaupel, R. Zander, and D. F. Bruley, eds. Plenum Press, New York and London, 1994, pp. 275–282.
- 8 L. Hoofd, J. Olders, and Z. Turek, Oxygen pressures calculated in a tissue volume with parallel capillaries, in *Oxygen Transport to Tissue-XII*, Advances in Experimental Medicine and Biology, vol. 277, J. Piiper, T. K. Goldstick, and M. Meyer, eds., Plenum Press, New York and London, 1990, pp. 21–29.
- 9 L. Hoofd, Z. Turek, and J. Olders, Calculation of oxygen pressures and fluxes in a flat plane perpendicular to any capillary distribution, in *Oxygen Transport to Tissue-XI*, Advances in Experimental Medicine and Biology, vol. 248, K. Rakušan, G. P. Biro, T. K. Goldstick, and Z. Turek, eds., Plenum Press, New York and London, 1989, pp. 187–196.
- 10 S. S. Kety, Determinants of tissue oxygen tension, *Fed. Proc.* 16:666–670 (1957).
- 11 A. S. Popel, Oxygen diffusion from capillary layers with concurrent flow, *Math. Biosci.* 50:171–193 (1980).
- 12 A. S. Popel, Theory of oxygen transport to tissue, *Crit. Rev. Biomed. Engrg.* 17:257–321 (1989).
- 13 J. F. O’Riordan and T. K. Goldstick, Examination of two models for oxygen equilibria, *Proc. Ann. Conf. Engrg. Med. Biol.* 27:235–236 (1985).
- 14 J. F. O’Riordan, T. K. Goldstick, L. N. Vida, G. R. Honig, and J. T. Ernest, Modeling whole blood oxygen equilibrium: Comparison of nine different models fitted to normal human blood, in *Oxygen Transport to Tissue-VII*, Advances in Experimental Medicine and Biology, vol. 191, F. Kreuzer, S. M. Cain, Z. Turek, and T. K. Goldstick, eds., Plenum Press, New York and London, 1985, pp. 505–522.